https://doi.org/10.15255/KUI.2022.059
KUI-46/2023
Original scientific paper
Received September 28, 2022
Accepted December 16, 2022

# Removal of Neonicotinoid Insecticides in a Flat-plate Photoreactor

*I. E. Zelić*,* *V. Tomašić*, and *Z. Gomzi*

University of Zagreb Faculty of Chemical Engineering and Technology, Department of Reaction Engineering and Catalysis, Trg Marka Marulića 19, 10 000 Zagreb, Croatia



**Abstract**

The aim of this study was to investigate the photolytic and photocatalytic degradation of neonicotinoids in an aqueous solution. Acetamiprid (ACE) and thiacloprid (TIA), two widely used insecticides, were used as model components. Experiments were performed in a flat-plate photoreactor under conditions of recirculation of the reaction mixture over an immobilised photocatalyst layer ($TiO_2$ modified by urea) using two artificial lamps for simulation of solar irradiation (2.4 % UVB and 12 % UVA; 300–700 nm). The catalyst used was characterised by XRD, UV/Vis-DRS, BET, SEM/EDX, and CHNS analysis. All experiments were performed at room temperature and atmospheric pressure, at a recirculation flow rate of 200 $cm^3\,min^{-1}$, and at an initial concentration of ACE and TIA of 10 $mg\,dm^{-3}$. For most measurements, the reaction mixture was sonicated for 15 min immediately before charging the reactor. The study focused on the influence of the pH of the initial solution on the efficiency of photocatalytic and photolytic degradation. It was found that photocatalytic degradation of the two model components was most effective under acidic operating conditions, *i.e.*, at pH 4.5, while photolysis resulted in their minimum degradation. It was also observed that pretreatment of the reaction mixture with ultrasound promoted photocatalytic degradation, while in the case of photolytic degradation, the application of ultrasound did not contribute to better degradation. Finally, photocatalytic degradation of TIA proved to be more successful than photodegradation of ACE (66.4 % *vs.* 25.8 %) under identical process conditions.

**Keywords**

*Heterogeneous catalysis, neonicotinoid insecticides, acetamiprid, thiacloprid, flate-plate photoreactor*

## 1 Introduction

Neonicotinoids are a relatively new and very popular class of insecticides that are currently registered in more than 120 countries around the world. Since their introduction in the late 1980s, the use of neonicotinoids has increased due to their unique mode of action and relatively low toxicity to non-target organisms and the environment.[1] Although a new generation of neonicotinoids has been developed in recent years, imidacloprid and thiacloprid with five-membered rings in their structure, thiamethoxam with a six-membered ring, and the four noncyclic compounds acetamiprid, clothianidin, dinotefuran, and nitenpyram have been widely used and studied. However, their high solubility in water and very slow degradation in the environment result in residues of neonicotinoids entering soil, sediments, groundwater, and surface waters. Despite their effectiveness in minimising crop damage, an increasing number of studies report adverse effects of neonicotinoids on humans, non-target insects, and aquatic invertebrates. In general, the excessive and uncontrolled use of neonicotinoids poses a risk to the entire ecosystem. Therefore, the European Union has placed five neonicotinoid insecticides, including acetamiprid and thiacloprid, on the Watch List, *i.e.*, a list of potentially hazardous pollutants.[2–5]

Due to increasing concentrations of neonicotinoid insecticides in surface and groundwater, advanced techniques and methods need to be developed to prevent bioaccumulation of insecticides and other undesirable persistent compounds in the environment, to enable their complete degradation, and ensure favourable conditions for environmental remediation. In the last decade, heterogeneous photocatalysis has attracted great attention as one of the advanced oxidation processes. Photocatalysis is a "green" and energy-saving technology with great potential. It can be applied to difficult-to-biodegrade, complex, and highly concentrated pollutants found in wastewater that cannot be degraded by classical water treatment methods. Titanium dioxide is one of the most widely used photocatalysts in many environmental applications due to its excellent physicochemical properties, such as low cost, high oxidation efficiency, chemical stability, high photostability, non-toxicity, recyclability, and availability.[6–8] Although $TiO_2$ has many desirable properties, its practical application in photocatalysis is severely limited due to a high carrier recombination rate and a relatively wide band gap ($\approx 3.0$ eV for rutile and $\approx 3.2$ eV for anatase), which only allows absorption of the ultraviolet component of sunlight (3–5 %). Considerable efforts have been made to improve the use of visible light by $TiO_2$ and to reduce the light-induced electron-hole recombination rate at the surface of $TiO_2$. As shown in Table 1, the most common strategies to affect the absorption range, include: i) photosensitising the semiconductor surface with organic dyes, ii) doping $TiO_2$ with metals, especially oxidation- and corrosion-resistant noble metals such as Au, Ag, and Pt, and iii) doping $TiO_2$ with non-metals (nitrogen, fluorine, sulphur, carbon, oxygen). Among all non-metallic dopants, doping with nitrogen has been the most studied due to its comparable atomic size, low ionisation energy, and stability.[9–14] Various physical and

* Corresponding author: Ivana Elizabeta Zelić, mag. ing. oecoing.
Email: izelic@fkit.unizg.hr
**Note:** The investigations in this paper were presented at the 9th International Conference WATER FOR ALL 2022, held on May 19–20, 2022, Osijek, Croatia.

*Table 1* – Illustration of possible strategies to improve the efficiency of the photocatalysts
*Tablica 1* – Ilustracija mogućih strategija za poboljšanje učinkovitosti fotokatalizatora

| Model pollutant<br>Onečišćujuća tvar | Photocatalyst<br>Fotokatalizator | Main outcomes<br>Glavni ishodi | Ref.<br>Lit. |
|---|---|---|---|
| Methylene blue (MB) | $TiO_2$ decorated with Ag nanoparticles, Ag@$TiO_2$ | Significantly enhanced and shifted absorption spectra towards the longer wavelength (450–550 nm) due to surface plasmon of silver nanoparticles. | 9 |
| Metilensko plavo | $TiO_2$ dekoriran nanočesticama Ag, Ag@$TiO_2$ | Znatno poboljšan i pomaknut apsorpcijski spektar prema višoj valnoj duljini (450–550 nm) zbog površinskog plazmona nanočestica srebra. | |
| 1H-benzotriazole (BT) | FeOOH@TiNT, $Fe_2O_3$@TiNT | Narrowing of band gaps of FeOOH@TiNT and $Fe_2O_3$@TiNT, depending on Fe concentration (1.85–3.19 eV) in comparison to TiNT (3.22 eV) | 10 |
| 1H-benzotriazol | | Sužavanje širine zabranjene zone FeOOH@TiNT i $Fe_2O_3$@TiNT ovisno o koncentraciji Fe (1,85 – 3,19 eV) u usporedbi s TiNT (3,22 eV). | |
| Different pollutants | Defective $TiO_2$ with oxygen vacancies | Coupling of nitrogen doping with oxygen vacancies formation inhibits the photogenerated charge carrier recombination, as well as enhances the visible light absorbance. | 12 |
| Različite onečišćujuće tvari | Defektivan $TiO_2$ s upražnjenim kisikovim mjestima | Povezivanje dopiranja dušikom s nastajanjem upražnjenih kisikovim mjestima inhibira rekombinaciju fotogeneriranih nositelja naboja i povećava apsorbanciju vidljive svjetlosti. | |
| Organic pollutants | Nitrogen-doped $TiO_2$ | Incorporation of nitrogen into the $TiO_2$ lattice leads to the formation of a new mid-gap energy state and decreases the gap of $TiO_2$ (to ≈ 2.5 eV). | 13 |
| Organski spojevi | $TiO_2$ dopiran dušikom | Ugradnja dušika u rešetku $TiO_2$ dovodi do nastajanja novog srednjeg energetskog stanja i smanjuje zabranjenu zonu $TiO_2$ (na ≈ 2,5 eV). | |
| Imidacloprid (IMI) | $TiO_2$ treated with $N_2$ plasma | The band gap of plasma-treated $TiO_2$ decreases compared to the unmodified $TiO_2$ (3.5 eV *vs.* 3.2 (anatase) and 3.0 (rutile). | 14 |
| Imidakloprid (IMI) | $TiO_2$ izložen plazmi $N_2$ | Zabranjena zona plazmom obrađenog $TiO_2$ smanjena je u usporedbi s nemodificiranim $TiO_2$ (3,5 eV *vs.* 3,2 (anataz) i 3,0 (rutil). | |

chemical methods have been used to introduce nitrogen into the $TiO_2$ crystal lattice, including ball milling, sputtering, plasma or ion implementation, sol-gel method, solvothermal method, hydrothermal method, direct hydrolysis of organic/inorganic salts, and oxidation of titanium nitride.[14] Ammonium chloride, guanidine hydrochloride, hydrazine, trimethylamine, urea, and many other organic compounds can be used as nitrogen sources. Urea is a hydrocarbon with high nitrogen content according to its molecular formula ($CH_4N_2O$), and is a potential additive for the preparation of nitrogen-doped titanium dioxide.[15]

The aim of this study was to modify the original $TiO_2$-P25 photocatalyst in a suitable way to reduce the band gap or energy gap between valence and conduction band ($E_g$), so that the photocatalyst can work efficiently under simulated solar irradiation. The studies were carried out in a flat-plate reactor with recirculation of the reaction mixture using an immobilised photocatalyst layer (nitrogen-doped $TiO_2$, N-$TiO_2$). The insecticides acetamiprid ($C_{10}H_{11}ClN_4$) and thiacloprid ($C_{10}H_9ClN_4S$) were used as model components, and the influence of the initial pH of the reaction mixture on the efficiency of photodegradation of acetamiprid and thiacloprid under the conditions of simulated solar radiation was investigated. Based on the obtained experimental data, the kinetics of heterogeneous photocatalytic degradation of the model components was studied and the model parameters estimated.

## 2 Experimental

### 2.1 Materials

All reagents were of analytical grade and used without further purification. The analytical standards acetamiprid and thiacloprid (PESTANAL™) (purity ≥ 98.0 %, ≤ 100 %) used for HPLC analysis were provided by Sigma Aldrich Company Ltd. Laboratory-grade acetamiprid, Boxer Mospilan 200 SP ($w$ = 20 %), was provided by Genera Inc., Kalinovica, Croatia. Ultrapure water (18.2 MΩ $cm^{-1}$) from a Nirosta Ultrapure Water System, Nirosta, Osijek, Croatia, was

used in this study to prepare solutions for the irradiation experiments. The initial pH values of the reaction mixture were adjusted with sulphuric acid ($H_2SO_4$) and sodium hydroxide (NaOH) supplied by VWR International S.A.S., Fontenay-sous-Bois, France. The photocatalyst, titanium dioxide ($TiO_2$-P25) nanopowder containing 80 % anatase and 20 % rutile with a primary particle size of 30–50 nm and a BET surface area of 50 $m^2\,g^{-1}$ was purchased from Evonik, Essen, Germany, and modified with urea (Kemika d. d., Zagreb, Croatia). The mineral binder Procol (Lasselsberger-Knauf d. o. o., Đurđevac, Croatia) was used to immobilise the photocatalyst. Formic acid 98 %, p.a. and HPLC-grade acetonitrile were purchased from VWR International, Radnor, Pennsylvania, USA.

### 2.2 Synthesis and characterisation of photocatalyst

Nitrogen-doped $TiO_2$ (N-$TiO_2$) was prepared by mechanically mixing urea as a nitrogen precursor with the $TiO_2$-P25 powder in a 4 : 1 ratio. Mechanical mixing was followed by heat treatment at atmospheric pressure and a temperature of 400 °C for 1 h. After cooling the mixture to room temperature, the resulting product was ground to a fine yellowish powder, which as such was ready for further immobilisation on an abrasive material used as a carrier. For immobilisation of the $TiO_2$ catalyst, a dense paste was prepared from 1.5 g of modified $TiO_2$, 0.5 g of commercial mineral binder (Procol), and 10 $cm^3$ of distilled water. After mixing, the paste was applied to the substrate in a thin layer using a brush. It was then dried at room temperature for 24 h. The immobilised layer thus prepared was adhered to the metal plate with double-sided adhesive tape so that it could be inserted into the photoreactor.

The $TiO_2$-P25 and N-$TiO_2$ catalysts used were characterised by several characterisation methods, including XRD, UV/Vis-DRS, BET, SEM /EDX, and CHNS analysis. X-ray powder diffraction (XRD) measurements were performed using a Shimadzu XRD 6000 diffractometer in the range $2\theta \approx 20–65°$ with Cu-Kα. UV-Vis diffuse reflectance spectra (UV-Vis DRS) were recorded using a Perkin-Elmer Lambda 35 UV/Vis spectrophotometer at room temperature in the wavelength range of 200–800 nm. The textural properties (specific surface area, total pore volume, and average pore diameter) were determined according to the Brunauer–Emmet–Teller model (BET) using a nitrogen adsorption device at 77 K (Micromeritics ASAP 2000). Scanning electron microscopy (SEM/EDX) images of the photocatalysts were acquired using an Oxford Instruments energy dispersive X-ray analyser EDS/INCA 350. The content of C, H, N, and S was determined using a Perkin-Elmer 2400 Series II CHNS analyser.

### 2.3 Experimental setup

Photodegradation experiments were performed in a 240 $cm^3$ plate photoreactor under recirculation conditions over an immobilised layer of nitrogen-doped $TiO_2$. Irradiation was performed with two commercial lamps (Arcadia, 8W, T5, 300 × 16 mm) simulating solar radiation (300–700 nm; 0.30–0.68 mW $cm^{-2}$), placed above the photoreactor. Light intensity was measured with a UVX radiometer (Labormed, Zagreb, Croatia) and with the appropriate sensors for UVA, UVB, and UVC radiation before and after the end of each experiment. Photocatalytic degradation of acetamiprid (ACE) and thiacloprid (TIA) at an initial concentration of 10 mg $dm^{-3}$ was performed at a recirculating flow rate of 200 $cm^3\,min^{-1}$. The structural formulas of ACE and TIA are shown in Fig. 1. Continuous circulation of the reaction mixture in the reaction chamber was achieved using a peristaltic pump (Masterflex® L/S®, Cole Parmer, USA). During the studies, the influence of pH (4.5–8.5) on the efficiency of photocatalytic degradation of the model components was investigated. The pH of the reaction mixture was adjusted by adding dilute aqueous solutions of NaOH and $H_2SO_4$. Immediately before filling the reactor, the reaction mixture was sonicated for 15 min in most measurements. The preceding ultrasonic (US) pretreatment resulted in a high degree of homogenisation of the reaction mixture. The solutions were kept in the dark in the presence of the photocatalyst for 30 min to allow the system to equilibrate. All experiments were performed at room temperature and atmospheric pressure. Samples (≈ 0.5 $cm^3$) were taken at specific time intervals during irradiation, taking into account that the total volume of the samples to be analysed was insignificant compared with the total volume of the reaction mixture in the reactor. Concentration and degradation rate were monitored by high-performance liquid chromatography (HPLC) using a UV-Vis detector at 254 nm. Separation and quantification were performed in an Agilent Zorbax C18 column using a mixture of water, acetonitrile, and formic acid as the mobile phase at a ratio of 95 : 5 : 0.3 (v%) and a flow rate of 1.0 $cm^3\,min^{-1}$ in gradient mode.

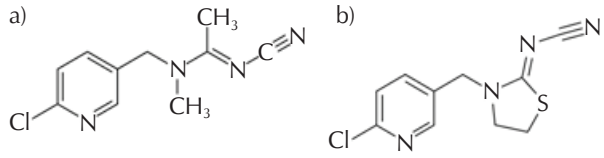


*Fig. 1* – Structural formula of: a) ACE and b) TIA
*Slika 1* – Strukturne formule molekula: a) ACE i b) TIA

## 3 Results and discussion

### 3.1 Characterisation of the powder photocatalyst

Due to the large band gap and high recombination rate of photoinduced electrons and holes, it is necessary to develop a method to improve the photocatalytic activity and extend the absorption edge of $TiO_2$ into the visible region. One way to achieve such improvements is to dope the semiconductor material with non-metals such as nitrogen. The XRD patterns of the $TiO_2$-P25 and N-$TiO_2$ catalysts are shown in Fig. 2. The XRD results indicate that the nitrogen precursor did not change the structure of the nitrogen-doped $TiO_2$, and the presence of nitrogen could not be confirmed.

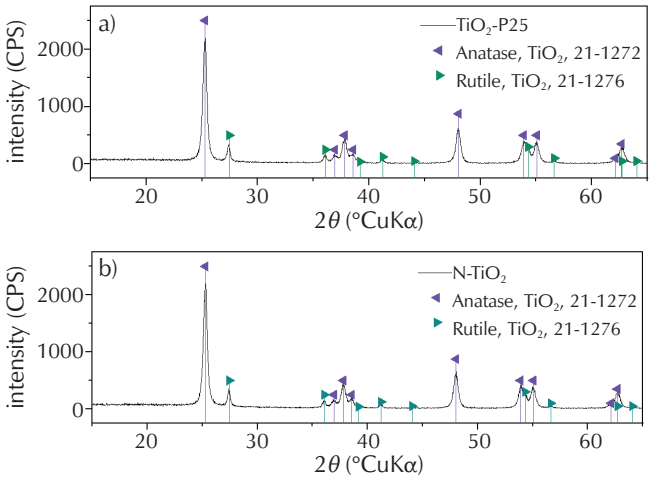


*Fig. 2* – XRD patterns of a) $TiO_2$-P25, and b) nitrogen-doped $TiO_2$ (N-$TiO_2$)
*Slika 2* – Rendgenski difraktogrami: a) $TiO_2$-P25 i b) dušikom-dopirani $TiO_2$ (N-$TiO_2$)

The optical absorption spectra of the measured samples are shown in Fig. 3. For N-$TiO_2$, a slight shift of the absorption edge to a lower energy in the visible light region was observed (Fig. 3a). The band gap energies were calculated using the Kubelka-Munk function by plotting $[F(R)E]^{1/2}$ *versus* the light energy, and correspond to 3.38 and 2.92 eV for $TiO_2$-P25 and N-$TiO_2$, respectively (Fig. 3b).

The BET surface area, pore size, and pore volume were estimated to be 56.0 $m^2 g^{-1}$, 15.2 nm, and 0.22 $cm^3 g^{-1}$ for N-$TiO_2$, respectively. These properties increased slightly in regard to $TiO_2$-P25, which had 53.6 $m^2 g^{-1}$, 10.4 nm, and 0.15 $cm^3 g^{-1}$ as BET surface area, pore size, and pore volume, respectively, indicating that N-$TiO_2$ could be useful for photodegradation. To investigate the chemical composition and chemical state of the catalysts, SEM/EDX analysis was performed. As listed in Table 2, $TiO_2$-P25 contained Ti, C, and O with atomic compositions of 33, 3, and 64 at.%, respectively. Results of SEM/EDX did not confirm the presence of nitrogen in the N-$TiO_2$, and the atomic compositions of Ti, C, and O were 29, 5, and 66 at.%, respectively.

Since EDX only measures the presence of nitrogen on the surface, CHNS elemental analysis was performed to provide secondary information on nitrogen content, which yielded a nitrogen content of 8.3 wt%.

### 3.2 Photodegradation measurements

Photolytic degradation of ACE and TIA was carried out at pH 4.5 in two ways: i) with ultrasound pretreatment of the reaction mixture, and ii) without ultrasound pretreatment.

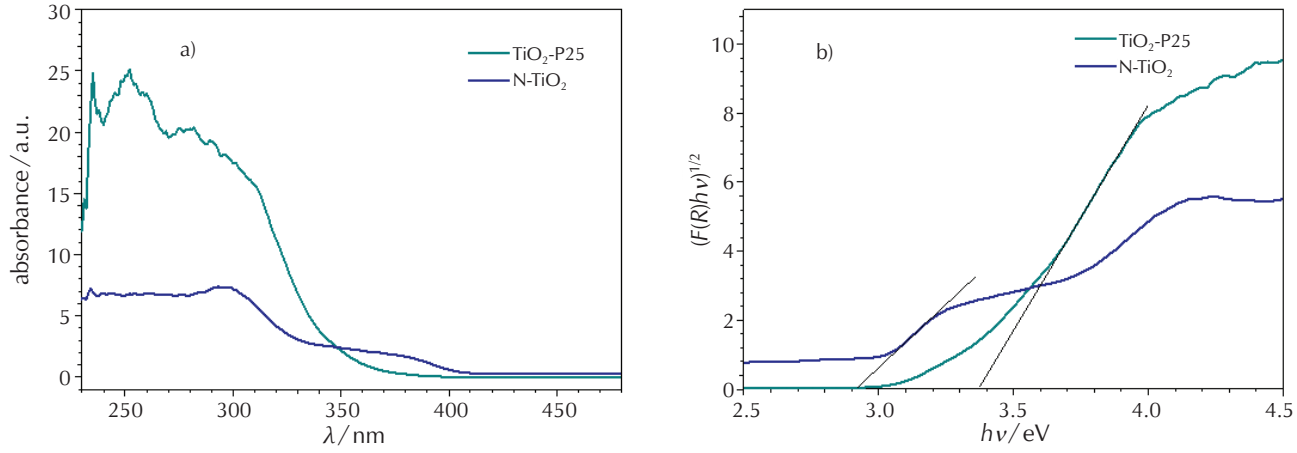


*Fig. 3* – UV/Vis absorption spectra of $TiO_2$-P25 and nitrogen-doped $TiO_2$ (N-$TiO_2$) (a), and corresponding Kubelka-Munk plots (b)
*Slika 3* – UV/Vis apsorpcijski spektri $TiO_2$-P25 i dušikom dopiranog $TiO_2$ (N-$TiO_2$) (a) te pripadajuće Kubelka-Munk funkcije (b)

*Table 2* – Results of SEM/EDX analysis
*Tablica 2* – Rezultati SEM/EDX analize

| Sample<br>Uzorak | Ti | | C | | O | |
|---|---|---|---|---|---|---|
| | Weight %<br>Maseni % | Atomic %<br>Atomski % | Weight %<br>Maseni % | Atomic %<br>Atomski % | Weight %<br>Maseni % | Atomic %<br>Atomski % |
| $TiO_2$-P25 | 59 | 33 | 1 | 3 | 40 | 64 |
| N-$TiO_2$ | 55 | 29 | 2 | 5 | 43 | 66 |

The results obtained are shown in Fig. 4. It was found that ultrasonic pretreatment of the reaction mixture slightly affected the obtained results. Photolytic degradation led to insignificant degradation of the stable model components, *i.e.,* the most important requirement for photodegradation of ACE and TIA is the presence of a suitable photocatalyst.

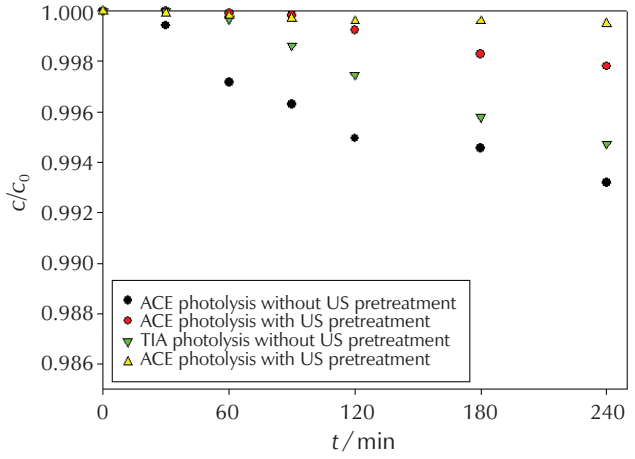


*Fig. 4* – Photolytic degradation of ACE and TIA. Reaction conditions: pH = 4.5, $c_0$ = 10 mg dm$^{-3}$, $q_R$ = 200 cm$^3$ min$^{-1}$, Arcadia lamps 8 W, $V_R$ = 240 cm$^3$.

*Slika 4* – Fotolitička razgradnja ACE i TIA. Reakcijski uvjeti: pH = 4,5, $c_0$ = 10 mg dm$^{-3}$, $q_R$ = 200 cm$^3$ min$^{-1}$, Arcadia lampe 8 W, $V_R$ = 240 cm$^3$.

To investigate the photocatalytic activity of nitrogen-doped $TiO_2$, the degradation of ACE and TIA was performed using two commercial lamps simulating solar radiation (Fig. 5). It could be observed that the presence of the photocatalyst greatly improved the degradation of the two pesticides compared to that without the photocatalyst. These results confirm the positive role of the use of N-$TiO_2$ for the degradation of pesticides. It was also found that pretreatment of the reaction mixture with ultrasound for a period of 15 min had a positive effect on the efficiency of photocatalytic degradation. A possible explanation for these results is the additional activation of the centres on the photocatalyst by the effect of ultrasound and the formation of additional reactive species (*e.g.,* hydroxyl radicals) by the ultrasound pretreatment of the reaction mixture. The maximum ACE and TIA removal efficiencies at an initial solution pH of 6.5 were 20.2 and 50.3 %, respectively. In conclusion, a nitrogen-doped $TiO_2$ photocatalyst was prepared by a relatively practical and environmentally friendly method using urea as a nitrogen source, which resulted in a reduction of $E_g$, and consequently, higher degradation rates of pesticides present in wastewater.

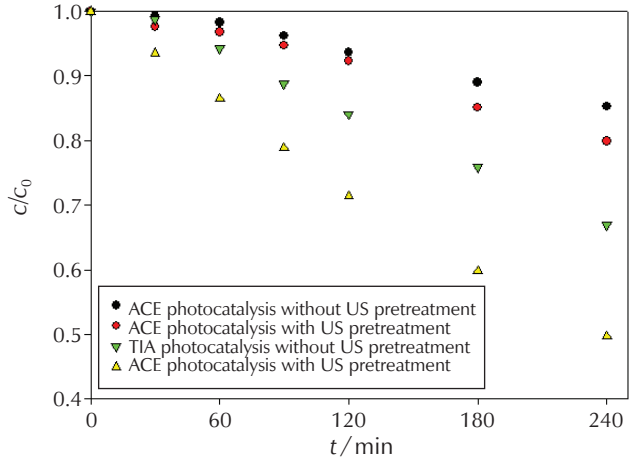


*Fig. 5* – Photocatalytic degradation of ACE and TIA. Reaction conditions: pH = 6.5, $c_0$ = 10 mg dm$^{-3}$, $q_R$ = 200 cm$^3$ min$^{-1}$, $P$ = 250 cm$^2$, Arcadia lamps 8 W, $V_R$ = 240 cm$^3$.

*Slika 5* – Fotokatalitička razgradnja ACE i TIA. Reakcijski uvjeti: pH = 6,5, $c_0$ = 10 mg dm$^{-3}$, $q_R$ = 200 cm$^3$ min$^{-1}$, $P$ = 250 cm$^2$, Arcadia lampe 8 W, $V_R$ = 240 cm$^3$.

In heterogeneous photocatalysis, pH has a significant effect on the photodegradation of organic pollutants. The surface charge of the photocatalyst depends on the pH of the reaction solution.[14] The interaction of the reactant molecule with the photocatalyst, the size of the $TiO_2$ particles, and the nature of the radicals and intermediates formed during photodegradation are strongly dependent on the pH, which also affects the adsorption of the reactant on the photocatalyst surface, and ultimately the efficiency of the process. In order to determine the optimal pH for performing photocatalytic decomposition, it is necessary to know the so-called point of zero charge (PZC). The PZC refers to the pH at which the surface of the photocatalyst has a net electrical charge of zero. Although the PZC for $TiO_2$ depends on the method of its preparation, a value of 6.25 is reported in the literature mainly for commercial $TiO_2$-P25.[15] From the results shown in Fig. 6, it could be concluded that, after 240 min of irradiation with Arcadia lamps used to simulate solar irradiation, the highest conversion of both ACE and TIA was obtained at a pH of 4.5–5.5, while no clear trend was observed at other pH values. The better degradation rate at a lower pH can be attributed to the fact that, at a pH of < 6.25, the $TiO_2$ surface is positively charged, while ACE is negatively charged at the same time due to the characteristic value of its dissociation constant of p$K_a$ = 4.16. This leads to a better adsorption of ACE on the surface of the photocatalyst, and thus to a more successful degradation.[16] No characteristic p$K_a$ values were found in the literature for TIA, which is reported not to dissociate or whose p$K_a$ is very low (0.01 +/− 0.1). It follows that TIA does not behave like an acid or alkali, *i.e.*, the efficiency of photocatalytic degradation cannot be related to the electrostatic interactions between TIA and $TiO_2$. Therefore, it is very difficult to predict theoretically the effects of pH on the photodegradation of TIA on a $TiO_2$ photocatalyst. However, the experimental results obtained in this work are in agreement with those published by Černigoj et al.[17] These authors reported the synergistic effect of ozone ($O_3$) and $TiO_2$ in the photodegradation of TIA in the acidic and neutral pH range, but the synergy disappeared in the alkaline range, which they attributed to the faster ozone degradation. The values of the estimated rate constants of photocatalytic degradation of ACE and TIA and the values of the root mean square deviation, RMSD, are shown in Table 3. The characteristic values for the rate

*Table 3* – Estimated values of the reaction rate constants, $k$, and the root mean square deviations, (RMSD), for ACE and TIA
*Tablica 3* – Procijenjene konstante brzine fotokatalitičke razgradnje ACE i TIA, $k$, i normalizirane vrijednosti korijena srednjeg kvadratnog odstupanja, RMSD

| | | pH = 4.5 | pH = 5.5 | pH = 6.5 | pH = 7.5 | pH = 8.5 |
|---|---|---|---|---|---|---|
| ACE | $k \cdot 10^3/\text{min}^{-1}$<br>RMSD | 1.16<br>0.0100 | 0.75<br>0.0467 | 0.86<br>0.0145 | 0.91<br>0.0130 | 0.87<br>0.0060 |
| TIA | $k \cdot 10^3/\text{min}^{-1}$<br>RMSD | 4.33<br>0.2072 | 3.65<br>0.1615 | 2.85<br>0.1101 | 3.25<br>0.1368 | 3.85<br>0.1786 |

constants k determined for TIA are higher than the corresponding values for ACE under identical operating conditions, indicating that TIA is degraded more successfully, *i.e.,* that its degradation results in higher conversions.

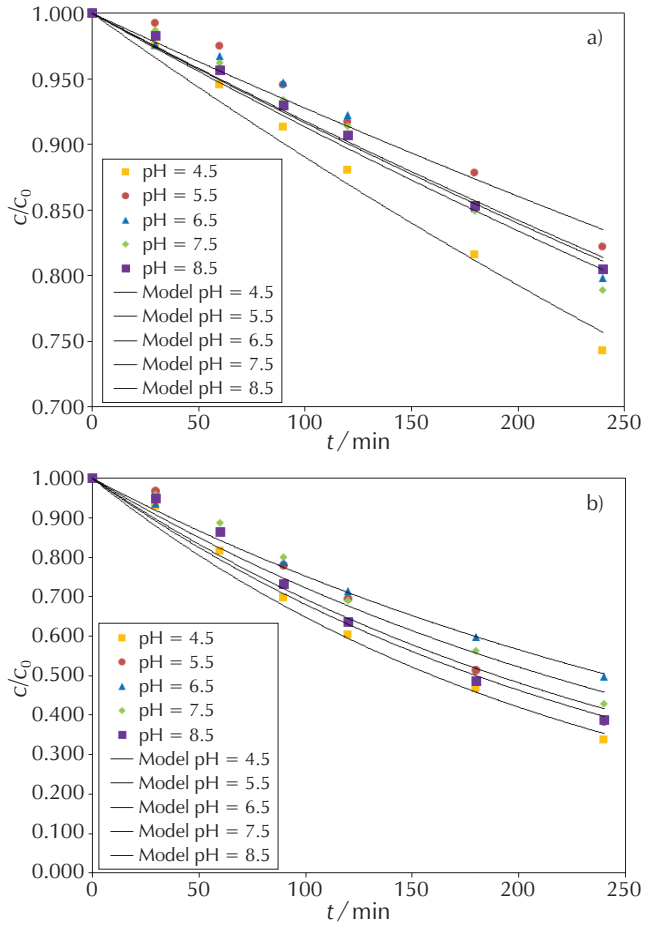


*Fig. 6* – Comparison of experimental results (points) with values obtained according to the assumed model (lines) at different initial reaction pH of a) ACE, and b) TIA. Reaction conditions: pH = 4.5–8.5, $c_0$ = 10 mg dm$^{-3}$, $q_R$ = 200 cm$^3$ min$^{-1}$, $P$ = 250 cm$^2$, Arcadia lamps 8 W, $V_R$ = 240 cm$^3$.
*Slika 6* – Usporedba eksperimentalnih rezultata (simboli) s teorijskim vrijednostima dobivenim prema pretpostavljenom modelu (linije) pri različitim početnim pH vrijednostima a) ACE i b) TIA. Reakcijski uvjeti: pH = 4,5 – 8,5, $c_0$ = 10 mg dm$^{-3}$, $q_R$ = 200 cm$^3$ min$^{-1}$, $P$ = 250 cm$^2$, Arcadia lampe 8 W, $V_R$ = 240 cm$^3$.

## 4 Conclusion

The aim of this study was to investigate the efficiency of nitrogen-doped $TiO_2$ in the form of an immobilised layer as a potential photocatalyst for the photocatalytic degradation of acetamiprid and thiacloprid in aqueous solutions under simulated solar irradiation. The nitrogen-doped $TiO_2$ was synthesised using low-cost urea as a nitrogen precursor. The N-doping shifted the energy band gap of $TiO_2$ to lower energy, *i.e.,* the absorption edge was shifted to the visible light region. The research focused on the effect of pH during photodegradation and was studied in a pH range of 4.5 to 8.5. In addition, the effect of pretreating the reaction mixture with ultrasound for 15 min on the photolytic and photocatalytic degradation results was investigated. The results of this study show that N-$TiO_2$ can efficiently catalyse the photodegradation of the insecticides acetamiprid and thiacloprid in the presence of simulated solar irradiation. The best degradation rate was obtained at pH 4.5, while pretreatment of the reaction mixture with ultrasound promoted photocatalytic degradation. Photocatalytic degradation of thiacloprid proved to be more successful than photodegradation of acetamiprid under the same process conditions.

ACKNOWLEDGEMENTS

This work was supported by the Croatian Science Foundation under the project INPhotoCat [IP-2018-01-8669]. The authors thank Res. Prof. Dr. Albin Pintar and co-workers from the National Institute of Chemistry for the $N_2$ adsorption-desorption measurements and CHNS elemental analysis of the samples studied.

### List of abbreviations and symbols
### Popis kratica i simbola

ACE – acetamiprid
– acetamiprid

BET – Brunauer–Emmet–Teller model
– Brunauer–Emmet–Teller model

$c$ – reactant concentration, mg dm$^{-3}$
– koncentracija reaktanta, mg dm$^{-3}$

$c_0$ – initial reactant concentration, mg dm$^{-3}$
– početna koncentracija reaktanta, mg dm$^{-3}$

$E_g$ – energy band gap, eV
– energija zabranjene vrpce, eV

HPLC – high-performance liquid chromatography
– tekućinska kromatografija visoke djelotvornosti

*k* – reaction rate constant, $min^{-1}$
– konstanta brzine reakcije, $min^{-1}$

N-$TiO_2$ – nitrogen-doped $TiO_2$
– dušikom dopirani $TiO_2$

PZC – point of zero charge
– točka nultog naboja

RMSD – root mean square deviations
– korijen srednjeg kvadratnog odstupanja

SEM/EDX – scanning electron microscopy
– skenirajuća elektronska mikroskopija

TIA – thiacloprid
– tiakloprid

$TiO_2$-P25 – commercial titanium dioxide
– komercijalno dostupan titanijev dioksid

US – ultrasonic
– ultrazvučni

UV – ultraviolet
– ultraljubičasto

UV/Vis DRS – UV/Vis diffuse reflectance spectra
– UV/Vis difuzna refleksijska spektroskopija

UVA – ultraviolet A
– ultraljubičasto A

UVB – ultraviolet B
– ultraljubičasto B

UVC – ultraviolet C
– ultraljubičasto C

*V* – volume, $dm^3$
– volumen, $dm^3$

XRD – X-ray powder diffraction
– difrakcija rendgenskih zraka

## References
## Literatura


1. *S. Hussain*, *C. J. Hartley*, *M. Shettigar*, *G. Pandey*, Bacterial biodegradation of neonicotinoid pesticides in soil and water systems, FEMS Microbiol. Lette. **363** (23) (2016) fnw252, doi: https://doi.org/10.1093/femsle/fnw252.
2. *J. M. Bonmatin, C. Giorio, V. Girolami, D. Goulson, D. P. Kreutzweiser, C. Krupke, M. Liess, E. Long, M. Marzaro, E. A. D. Mitchell, D. A. Noome, N. Simon-Delso, A. Tapparo*, Environmental fate and exposure; neonicotinoids and fipronil, Environ. Sci. Pollut. Res. **22** (2015) 35–45, doi: https://doi.org/10.1007/s11356-014-3332-7.
3. *L. Guo*, *W. W. Fang*, *L. L. Guo*, *C. F. Yao*, *Y. X. Zhao*, *F. Ge*, *Y. J. Dai*, Biodegradation of the neonicotinoid insecticide acetamiprid by actinomycetes *Streptomyces canus* CGMCC 13622 and characterization of the novel nitrile hydratase involved, J. Agric. Food Chem. **67** (2019) 5922–5924, doi: https://doi.org/10.1021/acs.jafc.8b06513.
4. *H. Jactel*, *F. Verheggen*, *D. Thiéry*, *A. J. Escobar-Gutiérrez*, *E. Gachet*, *N. Desneux*, Alternatives to neonicotinoids, Environ. Int. **129** (2019) 423–426, doi: https://doi.org/10.1016/j.envint.2019.04.045.
5. *W. S. Koe*, *J. W. Lee*, *W. C. Chong*, *Y. L. Pang*, *L. C. Sim*, An overview of photocatalytic degradation: photocatalysts, mechanisms, and development of photocatalytic membrane, Environ. Sci. aPollut. Res. **27** (3) (2020) 2522–2528, doi: https://doi.org/10.1007/s11356-019-07193-5.
6. *F. Jović*, *V. Tomašić*, Heterogena fotokataliza: osnove i primjena za obradu onečišćenog zraka, Kem. Ind. **60** (7-8) (2011) 387–403.
7. *Nasikhudin, M. Diantoro*, *A. Kusumaatmaja*, *K. Triyana*, Study on photocatalytic properties of $TiO_2$ nanoparticle in various pH conditions, J. Phys.: Conf. Series **1011** (2018) 012069, doi: https://doi.org/10.1088/1742-6596/1011/1/012069.
8. *M. Trochowski*, *M. Kobielusz*, *K. Mróz*, *M. Surówka*, *J. Hämäläinen*, *T. Iivonen*, *M. Leskelä*, *W. Macyk*, How insignificant modifications of photocatalysts can significantly change their photocatalytic activity, J. Mater. Chem. A **7** (43) (2019) 25142–25150, doi: https://doi.org/10.1039/c9ta09400h.
9. *M. M. Khan*, *S. A. Ansari*, *M. I. Amal*, *J. Lee*, *M. H. Cho*, Highly visible light active Ag@$TiO_2$ nanocomposites synthesized using an electrochemically active biofilm: a novel biogenic approach, Nanoscale **5** (10) (2013) 4427–4429, doi: https://doi.org/10.1039/c3nr00613a.
10. *T. Čižmar*, *V. Kojić*, *M. Rukavina*, *L. Brkljačić*, *K. Salamon*, *I. Grčić*, *L. Radetić*, *A. Gajović*, Hydrothermal synthesis of FeOOH and $Fe_2O_3$ modified self-organizing immobilized $TiO_2$ nanotubes for photocatalytic degradation of 1H-benzotriazole, Catalysts **10** (12) (2020) 1371, doi: https://doi.org/10.3390/catal10121371.
11. *T. Umebayashi*, *T. Yamaki*, *H. Itoh*, *K. Asai*, Band gap narrowing of titanium dioxide by sulfur doping, Appl. Phys. Lett. **81** (3) (2002) 454–455, doi: https://doi.org/10.1063/1.1493647.
12. *X. Pan*, *M. Yang*, *X. Fu*, *N. Zhang*, *Y. Xu*, Defective $TiO_2$ with oxygen vacancies: synthesis, properties and photocatalytic applications, Nanoscale **5** (9) (2013) 3601–3614, doi: https://doi.org/10.1039/c3nr00476g.
13. *S. A. Ansari*, *M. M. Khan*, *M. O. Ansari*, *M. H. Cho*, Nitrogen doped titanium dioxide (N-doped $TiO_2$) for visible light photocatalysis, New J. Chem. **40** (4) (2016) 3000–3007, doi: https://doi.org/10.1039/C5NJ03478G.
14. *K. Babić*, *V. Tomašić*, *V. Gilja*, *J. Le Cunff*, *V. Gomzi*, *A. Pintar*, *G. Žerjav*, *S. Kurajica*, *M. Duplančić*, *I. E. Zelić*, *T. Vukušić Pavičić*, *I. Grčić*, Photocatalytic degradation of imidacloprid in the flat-plate photoreactor under UVA and simulated solar irradiance conditions – The influence of operating conditions, kinetics and degradation pathway, J. Environ. Chem. Eng. **9** (4) (2021) 105611, doi: https://doi.org/10.1016/j.jece.2021.105611.
15. *N. Vela*, *G. Pérez-Lucas*, *J. Fenoll*, *S. Navarro*, Recent Overview on the Abatement of Pesticide Residues in Water by Photocatalytic Treatment Using $TiO_2$, in M. Janus (ed.), Application of Titanium Dioxide, IntechOpen, London, 2017, pp. 163.
16. *H. M. Coleman*, *B. R. Eggins*, *J. A. Byrne*, *F. L. Palmer*, *E. King*, Photocatalytic degradation of 17-β-oestradiol on immobilized $TiO_2$, Appl. Catal. B: Environ. **24** (1) (2000) L1–L5, doi: https://doi.org/10.1016/S0926-3373(99)00091-0.
17. *U. Černigoj, U. Lavrenčić Štangar*, *P. Trebše*, Degradation of neonicotinoid insecticides by different advanced oxidation processes and studying the effect of ozone on $TiO_2$ photocatalysis, Appl. Catal. B: Environ. **75** (3-4) (2007) 229–238, doi: https://doi.org/10.1016/j.apcatb.2007.04.014.

## SAŽETAK

### Razgradnja neonikotinoidnih insekticida u pločastom fotoreaktoru

*Ivana Elizabeta Zelić*,* *Vesna Tomašić* i *Zoran Gomzi*

Cilj ovog rada bio je ispitati fotolitičku i fotokatalitičku razgradnju neonikotinoida u vodenoj otopini. Acetamiprid (ACE) i tiakloprid (TIA), dva naširoko upotrebljavana insekticida, upotrijebljeni su kao modelne komponente. Istraživanja su provedena u pločastom fotoreaktoru u uvjetima recirkulacije reakcijske smjese primjenjujući imobilizirani sloj fotokatalizatora ($TiO_2$ modificiran ureom) uz dvije komercijalne lampe za simulaciju Sunčeva zračenja (2,4 % UVB i 12 % UVA; 300 – 700 nm). Upotrijebljeni katalizator karakteriziran je analizama XRD, UV/Vis-DRS, BET, SEM/EDX i CHNS. Sva mjerenja provedena su pri sobnoj temperaturi i atmosferskom tlaku, protoku recirkulacije od 200 $cm^3\,min^{-1}$ te uz konstantnu početnu koncentraciju ACE i TIA od 10 $mg\,dm^{-3}$. Tijekom većine mjerenja, reakcijska smjesa izložena je djelovanju ultrazvuka u vremenu od 15 min neposredno prije punjenja reaktora. Ispitan je utjecaj početne pH vrijednosti reakcijske smjese na učinkovitost fotokatalitičke i fotolitičke razgradnje. Nađeno je da je fotokatalitička razgradnja dviju modelnih komponenti najučinkovitija u kiselim uvjetima rada, tj. pri pH 4,5, dok je fotoliza rezultirala njihovom neznatnom razgradnjom. Također, ustanovljeno je da prethodna ultrazvučna obrada reakcijske smjese pospješuje fotokatalitičku razgradnju, dok u slučaju fotolitičke razgradnje primjena ultrazvuka ne pridonosi boljoj razgradnji. Konačno, utvrđeno je da je fotokatalitička razgradnja TIA učinkovitija od fotorazgradnje ACE (66.4 % *vs.* 25.8 %) pri jednakim radnim uvjetima.

**Ključne riječi**
*Heterogena kataliza, neonikotinoidni insekticidi, acetamiprid, tiakloprid, pločasti fotoreaktor*

*Sveučilište u Zagrebu Fakultet kemijskog inženjerstva i tehnologije, Zavod za reakcijsko inženjerstvo i katalizu, Trg Marka Marulića 19, 10 000 Zagreb*

Izvorni znanstveni rad
*Prispjelo 28. rujna 2022.*
*Prihvaćeno 16. prosinca 2022.*